


# Analysis of three-body charmed $B$ -meson decays under the factorization-assisted topological-amplitude approach

Si-Hong Zhou<sup>✉,\*</sup>, Run-Hui Li<sup>✉,†</sup> and Zheng-Yi Wei<sup>✉</sup>

*School of Physical Science and Technology, Inner Mongolia University, Hohhot 010021, China*

Cai-Dian Lü<sup>✉,‡</sup>

*Institute of High Energy Physics, CAS, Beijing 100049, China and School of Physics, University of Chinese Academy of Sciences, Beijing 100049, China*

 (Received 17 September 2021; accepted 29 November 2021; published 17 December 2021)

We analyze the quasi-two-body charmed  $B$  decays  $B_{(s)}^{+,0} \rightarrow D_{(s)}^* P_2 \rightarrow D_{(s)} P_1 P_2$  with  $P_{1,2}$  as a pion or kaon. The intermediate processes  $B_{(s)} \rightarrow D_{(s)}^* P_2$  are calculated with the factorization-assisted topological-amplitude approach, and the resonant effects are calculated with the Breit-Wigner formalism. Taking all  $P$ -wave resonance states  $\bar{D}_{(s)}^*$  into consideration, we present the related branching fractions, calculate the Breit-Wigner-tail effects, and investigate the flavor  $SU(3)$  breaking effects. Most of our branching fractions are consistent with the perturbative QCD approach's predictions as well as the current experimental data. With more precision calculation of the intermediate two-body charmed  $B$ -meson decays, our quasi-two-body  $B$  decays calculation has significantly less theoretical uncertainty than the perturbative QCD approach. Many of those channels without any experimental data will be confronted with the future more accurate experiment measurements. Our results of the Breit-Wigner-tail effects also agree with the experimental data very well. In  $B^0$  decays, this effect can reach approximately to 5%. It is also found that the Breit-Wigner tail effects are not sensitive to the widths of their corresponding resonances.

DOI: [10.1103/PhysRevD.104.116012](https://doi.org/10.1103/PhysRevD.104.116012)

## I. INTRODUCTION

$B$ -meson nonleptonic decays are very important for the study of many frontier topics, such as the mechanism of  $CP$  violation and the emergence of quantum chromodynamics. The three-body hadronic decays of  $B$  mesons, with many kinds of intermediate states parametrized by the sequential two-body decays, provide opportunities for the study of these common topics and of the hadron spectroscopy. So far, plenty of data on the three-body hadronic  $B$ -meson decays have been collected by *BABAR*, *Belle*, and *LHCb* experiments using the Dalitz plot technique, which induced a lot of theoretical studies.

On the theoretical side, contrary to two-body  $B$  decays, which have been analyzed extensively in the past two decades within the frameworks of the factorization approach, QCD factorization approach [1], perturbative

QCD (PQCD) [2], soft collinear effective theory [3], and some model-independent approaches such as the factorization-assisted topological-amplitude (FAT) approach [4], three-body  $B$  decays are more complicated. On one hand, the three-body decays receive both resonant and nonresonant contributions; on the other hand, factorization of these decays has not been completely proven. Some theoretical models aimed to calculate the nonresonant effects of some three-body  $B$  decays are in development, such as the heavy meson chiral perturbation theory [5–7], a model combining the heavy quark effective theory and chiral Lagrangian [8], and the perturbative QCD approach by introducing dimension distribution amplitudes [9]. The three-body  $B$ -meson decays are usually dominated by intermediate resonances. They proceed formally as quasi-two-body decays with an intermediate state of a vector or scalar resonance and a “bachelor” meson. The quasi-two-body framework is employed by the PQCD approach [9–16] and some phenomenological analysis based on factorization [5–7]. Some three-body  $B$  decays are also analyzed by the QCD factorization approach [17–19] and implemented within the  $U$ -spin, isospin, and flavor  $SU(3)$  symmetries (see also Refs. [20–25]).

In this work, we concentrate on three-body charmed  $B$  decays  $B_{(s)} \rightarrow D_{(s)} P_1 P_2$ , where  $P_{1,2}$  is a pion or kaon, via quasi-two-body decays  $B_{(s)} \rightarrow D_{(s)}^* P_2 \rightarrow D_{(s)} P_1 P_2$  with  $P_1$

\*shzhou@imu.edu.cn

†lirh@imu.edu.cn

‡lucd@ihep.ac.cn

*Published by the American Physical Society under the terms of the Creative Commons Attribution 4.0 International license. Further distribution of this work must maintain attribution to the author(s) and the published article's title, journal citation, and DOI. Funded by SCOAP<sup>3</sup>.*

stemming from the decay of the resonance and  $P_2$  representing a bachelor light meson. The Belle, BABAR, and LHCb Collaborations have achieved brilliant progress in identifying the excited charmed states and also found that their off-shell effects are indispensable [26–32]. The off-shell effect, also called the Breit-Wigner tail (BWT) effect, is the contribution when the pole mass of  $D_{(s)}^*$  is smaller than the invariant mass of  $D_{(s)}P_1$  or, in the other case, the contribution with the on-shell effect excluded by a cut on the invariant mass of  $D_{(s)}P_1$ . Recently, motivated by the experimental measurements on the off-shell effects of the  $D^*$  meson in  $B \rightarrow D\pi\pi(K)$  decays, theoretical attention has been paid to these virtual effects [14,33]. A new systematic research on the three-body charmed  $B$ -meson decays including  $D_{(s)}^*$  resonant states have been done subsequently in the PQCD approach [16]. About 5% off-shell contributions of  $D^*$  resonances and tiny contributions ( $<1\%$ ) from  $D_s^*$  resonances are found.

The theoretical uncertainty of the two-step process of  $B_{(s)} \rightarrow D_{(s)}^*P_2 \rightarrow D_{(s)}P_1P_2$  is dominated by the uncertainty from two-body nonleptonic  $B$  decays  $B_{(s)} \rightarrow D_{(s)}^*P$ . Large nonfactorizable contribution has been found in the factorization approach [34–36] and the PQCD approach [37,38]. Since the charm quark mass scale is also involved in these decays in addition to the  $b$  quark mass scale, the power corrections  $m_c/m_b$  of these decays are very difficult to calculate. In a previous work [39], two of us (S.-H. Z. and C.-D. L.), with other colleagues, utilize the framework of conventional topological diagram approach to group the decay amplitudes by different electroweak Feynman diagrams [40]. A global fit with all experimental data of these decays to extract the topological amplitudes including the nonfactorizable QCD contributions as well as the  $SU(3)$  breaking effects is performed. This so-called FAT approach [4,39,41–44] gives the most precise decay amplitudes of the two-body  $B$ -meson decays with charmed meson final states. For example, the amplitudes of the color-suppressed tree diagram (C) of Fig. 1(b), dominated by the nonfactorizable QCD effect, is larger in the FAT approach

than that in other approaches. In this paper, we apply the FAT approach to quasi-two-body  $B$ -meson decays, which will significantly reduce the theoretical uncertainty. The Breit-Wigner formalism is used to describe the resonance, and a strong coupling accounts for the subsequent decay  $D_{(s)}^* \rightarrow D_{(s)}P_1$ .

This paper is organized as follows. In Sec. II, the theoretical framework is introduced. The numerical results and discussions are collected in Sec. III. Section IV is a summary.

## II. FACTORIZATION OF AMPLITUDES FOR TOPOLOGICAL DIAGRAMS

Under the framework of quasi-two-body decay, the  $B_{(s)} \rightarrow D_{(s)}P_1P_2$  decay is divided into two stages.  $B_{(s)}$ -meson decays to  $D_{(s)}^*P_2$  first, and  $D_{(s)}^*$  decays to  $D_{(s)}P_1$  subsequently. The first decay  $B_{(s)} \rightarrow D_{(s)}^*P_2$  is a weak decay induced by  $b \rightarrow cq\bar{u}$  ( $q = d, s$ ) at quark level, and secondary decay  $D_{(s)}^* \rightarrow D_{(s)}P_1$  proceeds via strong interaction. In Fig. 1, we list the topological diagrams of these decays under the framework of quasi-two-body decay, including (a) the color-favored tree emission diagram  $T$ , (b) color-suppressed tree emission diagram  $C$ , and (c)  $W$ -exchange diagram  $E$ , which are specified by topological structures of the weak interaction. We will not consider processes induced by  $b \rightarrow uq\bar{u}$  ( $q = d, s$ ) transitions as they are Cabibbo-Kobayashi-Maskawa (CKM) matrix suppressed and there are not enough experimental data to do a global fit for their nonfactorizable contributions as done in the  $b \rightarrow c$  transition case.

The two-body charmless  $B$  decays have been proven factorization at high precision [3]. Large nonfactorizable contribution has been found in the two-body  $B$  decays with charmed meson final states [36,38], which we have illustrated in the fourth paragraph of the Introduction. The matrix elements for the topological diagram  $T$ ,  $C$ , and  $E$  ( $C$  and  $E$  include large nonfactorizable contribution) of  $B_{(s)} \rightarrow D_{(s)}^*P_2$ , derived by the FAT approach [39], are given as (see Eqs. (8), (9), and (10) of Ref. [39])

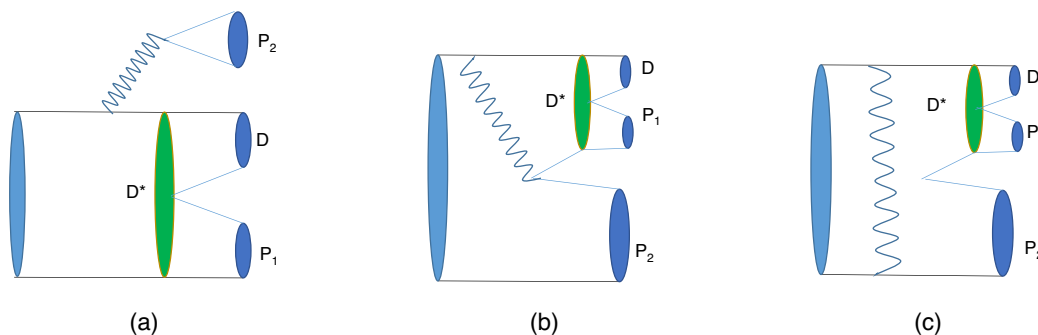


FIG. 1. Topological diagrams of  $B_{(s)} \rightarrow D_{(s)}^*P_2 \rightarrow D_{(s)}P_1P_2$  under the framework of quasi-two-body decay with the wave line representing a  $W$  boson: (a) the color-favored tree diagram  $T$ , (b) the color-suppressed tree diagram  $C$ , and (c) the  $W$ -exchange diagram  $E$ .

$$\begin{aligned}
T^{D^*P_2} &= \sqrt{2}G_F V_{cb} V_{uq}^* a_1(\mu) f_{P_2} m_{D^*} A_0^{B \rightarrow D^*}(m_{P_2}^2) (\epsilon_{D^*}^* \cdot p_B), \\
C^{D^*P_2} &= \sqrt{2}G_F V_{cb} V_{uq}^* f_{D^*} m_{D^*} F_1^{B \rightarrow P_2}(m_{D^*}^2) (\epsilon_{D^*}^* \cdot p_B) \chi^C e^{i\phi^C}, \\
E^{D^*P_2} &= \sqrt{2}G_F V_{cb} V_{uq}^* m_{D^*} f_B \frac{f_{D^*} f_{P_2}}{f_D f_\pi} \chi^E e^{i\phi^E} (\epsilon_{D^*}^* \cdot p_B). \quad (1)
\end{aligned}$$

In these equations, for simpler notation, the subscript (s) in  $D^*$  has been kept only in  $f_{D^*}$ . This notation is also applied in the following equations involving  $D^*$ , such as Eqs. (3), (4), and (6).  $\epsilon_{D^*}^*$  is the polarization vector of the  $D^*$ .  $f_{P_2}$  and  $f_{D^*}$  are the decay constants of the corresponding meson  $P_2$  and  $D^*$ .  $A_0^{B \rightarrow D^*}(m_{P_2}^2)$  and  $F_1^{B \rightarrow P_2}(s)$  stand for the vector form factors of  $B_{(s)} \rightarrow D^*$  and  $B_{(s)} \rightarrow P_2$  transitions. The form factors are  $Q^2$  dependent, and we use the expression in the pole model,

$$F_i(Q^2) = \frac{F_i(0)}{1 - \alpha_1 \frac{Q^2}{m_{\text{pole}}^2} + \alpha_2 \frac{Q^4}{m_{\text{pole}}^4}}, \quad (2)$$

where  $F_i$  represents  $F_1$  and  $A_0$  and  $m_{\text{pole}}$  is the mass of the corresponding pole state, such as  $B$  for  $A_0$ , and  $B^*$  for  $F_1$ .  $a_1(\mu)$  is the effective Wilson coefficient for the factorizable emission diagram  $T$ .  $\chi^{C(E)}$  and  $\phi^{C(E)}$  denote the magnitude and associate phase of  $C(E)$  diagram, which are universal and are extracted from the experimental data.

The intermediate vector  $D^*_{(s)}$  resonance is described by the Breit-Wigner formalism [7],

$$R(s) = \frac{1}{s - m_{D^*}^2 + im_{D^*} \Gamma_{D^*}(s)}, \quad (3)$$

where the invariant mass square  $s = (p_D + p_1)^2$  with  $p_D$  and  $p_1$  denoting the 4-momenta of the  $D$  and  $P_1$  mesons, respectively. The width of the  $D^*$  meson is energy dependent [30],

$$\Gamma_{D^*}(s) = \Gamma_0 \left( \frac{q}{q_0} \right)^3 \left( \frac{m_{D^*}}{\sqrt{s}} \right) X^2(qr_{\text{BW}}). \quad (4)$$

The Blatt-Weisskopf barrier factor is given as [45]

$$X(qr_{\text{BW}}) = \sqrt{[1 + (q_0 r_{\text{BW}})^2] / [1 + (qr_{\text{BW}})^2]} \quad (5)$$

with barrier radius  $r_{\text{BW}} = 4.0 \text{ GeV}^{-1}$  [27,28,30]. The magnitude  $q$  of the momentum is  $q = \frac{1}{2} \sqrt{[s - (m_D + m_{P_1})^2][s - (m_D - m_{P_1})^2] / s}$  of the final state  $D_{(s)}$  or  $P_1$  in the rest frame of the  $D^*$ . The momentum  $q_0$  is the value of  $q$  when the invariant mass is equal to the pole mass of the resonance,  $s = m_{D^*}^2$ . When a pole mass is

located outside the kinematics region, e.g.,  $m_{D^*} < m_D + m_{P_1}$ , it will be replaced with an effective mass,  $m_{D^*}^{\text{eff}}$ , given by the *ad hoc* formula [30,46,47],

$$\begin{aligned}
m_{D^*}^{\text{eff}}(m_{D^*}) \\
= m^{\text{min}} + (m^{\text{max}} - m^{\text{min}}) \left[ 1 + \tanh \left( \frac{m_{D^*} - \frac{m^{\text{min}} + m^{\text{max}}}{2}}{m^{\text{max}} - m^{\text{min}}} \right) \right], \quad (6)
\end{aligned}$$

where  $m^{\text{max}}$  and  $m^{\text{min}}$  are the upper and lower boundaries of the kinematics region, respectively. The width  $\Gamma_0$  is the full width of a resonance  $D^*$ , i.e., the width in Eq. (4) when  $s = m_{D^*}^2$ . The full width of charged resonance is measured as  $\Gamma(D^{*+}) = 83.4 \pm 1.8 \text{ keV}$  [48]. There is no measurement for the neutral  $D^*$  meson, and we will use the theoretical value obtained by the light-cone sum rules  $\Gamma(D^{*0}) = 55.4 \pm 1.4 \text{ keV}$  [49]. There is no direct experimental measurement for the full width of the  $D_s^*$  meson [48]. On the theoretical side, large discrepancies exist, such as  $\Gamma_{D_s^* \rightarrow D_s \gamma} = 0.066 \pm 0.026 \text{ keV}$  in lattice QCD [50],  $\Gamma_{D_s^* \rightarrow D_s \gamma} = 0.59 \pm 0.15 \text{ keV}$  in QCD sum rules [51], and  $\Gamma_{D_s^* \rightarrow D_s \pi^0} = 8.1_{-2.6}^{+3.0} \text{ eV}$  in heavy meson chiral perturbation [52]. Therefore, we will use the value of 1 keV to include the largest uncertainty. To be more clear, the full widths of these resonance states  $D^*_{(s)}$ , in addition to their masses, are listed in Table I.

The strong decay  $\langle P_1(p_1) D(p_D) | D^*(p^*) \rangle$  with the momentum of  $D^*$  denoted by  $p^*$  is parametrized as a strong coupling constant  $g_{D^* D P_1}$ , which can be extracted from the partial width  $\Gamma_{D^*_{(s)} \rightarrow D_{(s)} P_1}$  by

$$\Gamma_{D^*_{(s)} \rightarrow D_{(s)} P_1} = \frac{P_{P_1}^3}{24\pi m_{D^*_{(s)}}^2} g_{D^*_{(s)} D_{(s)} P_1}^2. \quad (7)$$

$g_{D^* D \pi}$  is determined precisely as  $g_{D^* D \pi} = 16.92 \pm 0.13 \pm 0.14$  [53,54] by using the isospin relation  $g_{D^* D^0 \pi^+} = -\sqrt{2} g_{D^* D^+ \pi^0}$  and the total decay width of the  $D^{*+}$ . The other strong couplings can be related with  $g_{D^* D \pi}$  through the universal coupling  $\hat{g}$  [53,55],

$$\hat{g} = \frac{g_{D^* D \pi(K)} f_\pi}{2\sqrt{m_{D^*}^* m_D}} = \frac{g_{D^* D K} f_K}{2\sqrt{m_{D^*}^* m_D}}. \quad (8)$$

TABLE I. The masses (MeV) and full widths (KeV) of resonance states  $D^*_{(s)}$ .

$m_{D^{*\pm}}$	$m_{D^{*0}}$	$m_{D_s^{*\pm}}$	$\Gamma_{D^{*\pm}}$	$\Gamma_{D^{*0}}$	$\Gamma_{D_s^{*\pm}}$
2010	2007	2112	$83.4 \pm 1.8$	$55.4 \pm 1.4$	1

With this universal relation, one gets  $g_{D_s^*DK} = 14.6 \pm 0.06 \pm 0.07$  and  $g_{D^*D_sK} = 14.6 \pm 0.10 \pm 0.13$ , which agree very well with the values  $g_{D_s^*DK} = 14.6 \pm 1.7$  and  $g_{D^*D_sK} = 14.7 \pm 1.7$  measured by the CLEO Collaboration [56] and  $g_{D_s^*DK} = 15.2$  and  $g_{D^*D_sK} = 15.2$  calculated by the quark model [57].

Combing them together, the decay amplitudes of each topological diagrams shown in Fig. 1 are given as

$$\begin{aligned} T &= \langle P_1(p_1)D(p_D)|(\bar{c}b)_{V-A}|B(p_B)\rangle \langle P_2(p_2)|(\bar{q}u)_{V-A}|0\rangle \\ &= \frac{\langle P_1(p_1)D(p_D)|D^*(p^*)\rangle}{s - m_{D^*}^2 + im_{D^*}\Gamma_{D^*}(s)} \langle D^*(p^*)|(\bar{c}b)_{V-A}|B(p_B)\rangle \langle P_2(p_2)|(\bar{q}u)_{V-A}|0\rangle \\ &= p_2 \cdot (p_1 - p_D) \sqrt{2} G_F V_{cb} V_{uq}^* f_{P_2} m_{D^*} A_0^{BD^*}(m_{P_2}^2) a_1(\mu) \frac{g_{D^*DP_1}}{s - m_{D^*}^2 + im_{D^*}\Gamma_{D^*}(s)}, \end{aligned} \quad (9)$$

$$\begin{aligned} C &= \langle P_1(p_1)D(p_D)|(\bar{c}u)_{V-A}|0\rangle \langle P_2(p_2)|(\bar{q}b)_{V-A}|B(p_B)\rangle \\ &= \frac{\langle P_1(p_1)D(p_D)|D^*(p^*)\rangle}{s - m_{D^*}^2 + im_{D^*}\Gamma_{D^*}(s)} \langle D^*(p^*)|(\bar{c}u)_{V-A}|0\rangle \langle P_2(p_2)|(\bar{q}b)_{V-A}|B(p_B)\rangle \\ &= p_2 \cdot (p_1 - p_D) \sqrt{2} G_F V_{cb} V_{uq}^* f_{D^*} m_{D^*} F_1^{BP_2}(p^*) \chi^C e^{i\phi^C} \frac{g_{D^*DP_1}}{s - m_{D^*}^2 + im_{D^*}\Gamma_{D^*}(s)}, \end{aligned} \quad (10)$$

$$\begin{aligned} E &= \langle P_1(p_1)D(p_D)P_2(p_2)|\mathcal{H}_{\text{eff}}|B(p_B)\rangle \\ &= \frac{\langle P_1(p_1)D(p_D)|D^*(p^*)\rangle}{s - m_{D^*}^2 + im_{D^*}\Gamma_{D^*}(s)} \langle D^*(p^*)P_2(p_2)|\mathcal{H}_{\text{eff}}|B(p_B)\rangle \\ &= p_2 \cdot (p_1 - p_D) \sqrt{2} G_F V_{cb} V_{uq}^* f_B m_{D^*} \frac{f_{D^*} f_{P_2}}{f_\pi f_D} \chi^E e^{i\phi^E} \frac{g_{D^*DP_1}}{s - m_{D^*}^2 + im_{D^*}\Gamma_{D^*}(s)}. \end{aligned} \quad (11)$$

where  $p^* = p_1 + p_D$ .

The total decay amplitude of  $B_{(s)} \rightarrow D_{(s)} P_1 P_2$  can be written as

$$\begin{aligned} &\langle D_{(s)}(p_D)P_1(p_1)P_2(p_2)|\mathcal{H}_{\text{eff}}|B_{(s)}(p_B)\rangle \\ &= p_2 \cdot (p_1 - p_D) \mathcal{A}(s), \end{aligned} \quad (12)$$

where  $\mathcal{A}(s)$  represents the summation of amplitudes in Eq. (9)–(11) with the factor  $p_2 \cdot (p_1 - p_D)$  taken out. The differential width of  $B_{(s)} \rightarrow D_{(s)} P_1 P_2$  is

$$d\Gamma = ds \frac{1}{(2\pi)^3} \frac{(|\mathbf{p}_1||\mathbf{p}_2|)^3}{24m_B^3} |\mathcal{A}(s)|^2, \quad (13)$$

where  $|\mathbf{p}_1|$  and  $|\mathbf{p}_2|$  represent the magnitudes of the momentum  $p_1$  and  $p_2$ , respectively. In the rest frame of the  $D_{(s)}^*$  resonance, their expressions are

$$\begin{aligned} |\mathbf{p}_1| &= \frac{1}{2\sqrt{s}} \sqrt{[s - (m_D + m_{P_1})^2][s - (m_D - m_{P_1})^2]}, \\ |\mathbf{p}_2| &= \frac{1}{2\sqrt{s}} \sqrt{[(m_B^2 - m_{P_2}^2)^2] - 2(m_B^2 + m_{P_2}^2)s + s^2}, \end{aligned} \quad (14)$$

where  $|\mathbf{p}_1| = q$ .

### III. NUMERICAL RESULTS AND DISCUSSION

The input parameters in this work contain the CKM matrix elements, decay constants, transition form factors, Wilson coefficients, and nonperturbative parameters of  $C(E)$  topological diagrams  $\chi^{C(E)}$  and  $\phi^{C(E)}$ . We use Wolfenstein parametrization of the CKM matrix with the Wolfenstein parameters as [48]

$$\begin{aligned} \lambda &= 0.22650 \pm 0.00048, & A &= 0.790_{-0.012}^{+0.017}, \\ \bar{\rho} &= 0.141_{-0.017}^{+0.016}, & \bar{\eta} &= 0.357 \pm 0.01, \end{aligned}$$

which lead to  $V_{cb}V_{ud}^* = 0.0395_{-0.0006}^{+0.0009}$  and  $V_{cb}V_{us}^* = 0.0092 \pm 0.0002$ . The decay constants of light pseudoscalar mesons and vector charm mesons  $D_{(s)}^*$  and transition form factors of  $B$ -meson decays at recoil momentum square  $Q^2 = 0$  are listed in Tables II and III, respectively. The decay constants of  $\pi$ ,  $K$ ,  $D$ , and  $B$  from the particle data group are used [48]. There are no experimental data for decay constants of  $D_s$ ,  $D_{(s)}^*$ , and  $B_s$  and all form factors used here. Here, we use the same theoretical values as in the previous work by two of us (S.-H. Z. and C.-D. L.) with other colleagues [39], with 5% uncertainty kept for decay constants and 10% uncertainty for form factors. Similarly,

TABLE II. The decay constants of light pseudoscalar mesons and vector mesons (in units of MeV).

$f_\pi$	$f_K$	$f_D$	$f_{D_s}$	$f_{D^*}$	$f_{D_s^*}$	$f_B$	$f_{B_s}$
$130.2 \pm 1.7$	$155.6 \pm 0.4$	$211.9 \pm 1.1$	$258 \pm 12.5$	$220 \pm 11$	$270 \pm 14$	$190.9 \pm 4.1$	$225 \pm 11.2$

TABLE III. The transition form factors at  $Q^2 = 0$  and dipole model parameters used in this work.

	$F_1^{B \rightarrow \pi}$	$F_1^{B \rightarrow K}$	$F_1^{B_s \rightarrow K}$	$A_0^{B \rightarrow D^*}$	$A_0^{B_s \rightarrow D_s^*}$
$F(0)$	0.28	0.33	0.29	0.56	0.57
$\alpha_1$	0.52	0.54	0.57	2.44	2.49
$\alpha_2$	0.45	0.50	0.50	1.98	1.74

we will also use the dipole parametrization to describe the  $Q^2$  dependence of form factors.

The Wilson coefficients  $C_1$  and  $C_2$  at scale  $\mu = m_b/2$  are  $-0.287$  and  $1.132$ , respectively. Then, the effective Wilson coefficients  $a_1$  is  $1.036$ . The nonperturbative contribution parameters  $\chi^{C(E)}$  and  $\phi^{C(E)}$  extracted from experimental data by the fit performed in Ref. [39] are

$$\begin{aligned} \chi^C &= 0.48 \pm 0.01, & \phi^C &= (56.6_{-3.8}^{+3.2})^\circ, \\ \chi^E &= 0.024_{-0.001}^{+0.002}, & \phi^E &= (123.9_{-2.2}^{+3.3})^\circ. \end{aligned} \quad (15)$$

With all the inputs, the branching fractions of  $B^{0,+} \rightarrow \bar{D}_{(s)}^* P_2 \rightarrow \bar{D}_{(s)} P_1 P_2$  and  $B_s^0 \rightarrow \bar{D}_{(s)}^* P_2 \rightarrow \bar{D}_{(s)} P_1 P_2$  can be obtained by integrating the differential width in Eq. (13) over the kinematics region. Our numerical results for  $B^{0,+}$  and  $B_s^0$  decays are collected in Tables IV and V, respectively. In our results, the errors are estimated with 5% variations of form factors, 10% variations of decay constants, and the uncertainties of the other nonperturbative parameters. One can see that the dominating errors are from the uncertainties of form factors. In the tables, we also list the intermediate decays as well as the topological contributions represented by the corresponding symbols.

### A. Hierarchy of branching fraction

The hierarchies of branching fractions can be seen clearly in the last columns of Tables IV and V. First, let us pay attention to those decays in Table IV whose intermediate states can be changed to each other by swapping the bachelor light mesons pion with a kaon,

TABLE IV. The branching ratios of quasi-two-body decays  $B_{u,d} \rightarrow D_{(s)}^* P_2 \rightarrow D_{(s)} P_1 P_2$ . The decays with on-shell effects are denoted by  $\mathcal{B}$ , and those without on-shell effects are denoted by  $\mathcal{B}_v$ . The characters  $T$ ,  $C$  and  $E$  represent the corresponding topological contributions. The uncertainties are from form factors, decay constants and nonperturbative parameters, respectively.

Decay modes	Amplitudes	$\mathcal{B}$ or $\mathcal{B}_v$	Results	Units
$B^0 \rightarrow D^{*-} \pi^+ \rightarrow \bar{D}^0 \pi^- \pi^+$	T + E	$\mathcal{B}$	$1.77_{-0.35-0.05-0.01}^{+0.39+0.05+0.01}$	$10^{-3}$
			$8.03_{-1.57-0.22-0.04}^{+1.74+0.22+0.07}$	$10^{-4}$
			$1.64_{-0.32-0.04-0.01}^{+0.36+0.05+0.01}$	$10^{-5}$
$B^0 \rightarrow D^{*-} K^+ \rightarrow \bar{D}^0 \pi^- K^+$	T	$\mathcal{B}$	$1.47_{-0.28-0.08-0}^{+0.31+0.08+0}$	$10^{-4}$
			$6.63_{-1.26-0.03-0}^{+1.39+0.03+0}$	$10^{-5}$
			$1.28_{-0.24-0.01-0}^{+0.27+0.01+0}$	$10^{-6}$
$B^0 \rightarrow \bar{D}^{*0} \pi^0 \rightarrow \bar{D}^0 \pi^0 \pi^0$	$\frac{1}{\sqrt{2}}(E - C)$	$\mathcal{B}$	$1.39_{-0.27-0.14-0.07}^{+0.30+0.14+0.07}$	$10^{-4}$
			$1.07_{-0.21-0.10-0.05}^{+0.23+0.10+0.05}$	$10^{-5}$
			$1.60_{-0.31-0.16-0.08}^{+0.35+0.16+0.08}$	$10^{-6}$
$B^0 \rightarrow \bar{D}^{*0} K^0 \rightarrow \bar{D}^0 \pi^0 K^0$	C	$\mathcal{B}$	$2.23_{-0.42-0.22-0.09}^{+0.47+0.23+0.09}$	$10^{-5}$
			$1.67_{-0.32-0.16-0.07}^{+0.35+0.17+0.07}$	$10^{-6}$
			$2.38_{-0.45-0.23-0.10}^{+0.50+0.24+0.10}$	$10^{-7}$
$B^+ \rightarrow \bar{D}^{*0} \pi^+ \rightarrow \bar{D}^0 \pi^0 \pi^+$	T + C	$\mathcal{B}$	$3.09_{-0.47-0.01-0.09}^{+0.51+0.01+0.08}$	$10^{-3}$
			$2.27_{-0.34-0.07-0.06}^{+0.37+0.07+0.06}$	$10^{-4}$
			$3.21_{-0.48-0.10-0.10}^{+0.52+0.11+0.09}$	$10^{-5}$
$B^+ \rightarrow \bar{D}^{*0} K^+ \rightarrow \bar{D}^0 \pi^0 K^+$	T + C	$\mathcal{B}$	$2.35_{-0.36-0.06-0.07}^{+0.39+0.06+0.06}$	$10^{-4}$
			$1.69_{-0.26-0.04-0.05}^{+0.28+0.04+0.04}$	$10^{-5}$
			$2.29_{-0.35-0.06-0.07}^{+0.37+0.06+0.06}$	$10^{-6}$

TABLE V. The same as Table IV, but for the quasi-two-body  $B_s^0 \rightarrow D_{(s)}^* P_2 \rightarrow DP_1 P_2$  decays.

Decay modes	Amplitudes	$\mathcal{B}$ or $\mathcal{B}_v$	Results	Units
$B_s^0 \rightarrow D_s^{*-} \pi^+ \rightarrow \bar{D}^0 K^- \pi^+$ $\rightarrow D^- \bar{K}^0 \pi^+$	T	$\mathcal{B}_v$	$4.21^{+0.88+0.11+0}_{-0.80-0.11-0}$	$10^{-5}$
		$\mathcal{B}_v$	$4.07^{+0.85+0.11+0}_{-0.77-0.11-0}$	$10^{-5}$
$B_s^0 \rightarrow D_s^{*-} K^+ \rightarrow \bar{D}^0 K^- K^+$ $\rightarrow D^- \bar{K}^0 K^+$	T + E	$\mathcal{B}_v$	$2.84^{+0.62+0.02+0.03}_{-0.56-0.02-0.02}$	$10^{-6}$
		$\mathcal{B}_v$	$2.74^{+0.60+0.02+0.03}_{-0.54-0.02-0.02}$	$10^{-6}$
$B_s^0 \rightarrow D^{*-} \pi^+ \rightarrow \bar{D}^0 \pi^- \pi^+$ $\rightarrow D^- \pi^0 \pi^+$ $\rightarrow D_s^- K^0 \pi^+$	E	$\mathcal{B}$	$5.98^{+0+0.87+1.04}_{-0-0.83-0.49}$	$10^{-7}$
		$\mathcal{B}$	$2.71^{+0+0.39+0.47}_{-0-0.37-0.22}$	$10^{-7}$
		$\mathcal{B}_v$	$5.80^{+0+0.84+1.01}_{-0-0.80-0.47}$	$10^{-9}$
$B_s^0 \rightarrow \bar{D}^{*0} \pi^0 \rightarrow \bar{D}^0 \pi^0 \pi^0$ $\rightarrow D^- \pi^+ \pi^0$ $\rightarrow D_s^- K^+ \pi^0$	$\frac{1}{\sqrt{2}} E$	$\mathcal{B}$	$2.76^{+0+0.30+0.36}_{-0-0.28-0.17}$	$10^{-7}$
		$\mathcal{B}_v$	$2.03^{+0+0.40+0.48}_{-0-0.38-0.23}$	$10^{-8}$
		$\mathcal{B}_v$	$2.91^{+0+0.42+0.50}_{-0-0.40-0.24}$	$10^{-9}$
$B_s^0 \rightarrow \bar{D}^{*0} \bar{K}^0 \rightarrow \bar{D}^0 \pi^0 \bar{K}^0$ $\rightarrow D^- \pi^+ \bar{K}^0$ $\rightarrow D_s^- K^+ \bar{K}^0$	C	$\mathcal{B}$	$3.40^{+0.71+0.35+0.14}_{-0.65-0.33-0.14}$	$10^{-4}$
		$\mathcal{B}_v$	$2.61^{+0.55+0.27+0.11}_{-0.50-0.26-0.11}$	$10^{-5}$
		$\mathcal{B}_v$	$3.88^{+0.81+0.40+0.16}_{-0.74-0.38-0.16}$	$10^{-6}$

e.g.,  $B^0 \rightarrow D^{*-} \pi^+ \rightarrow \bar{D}^0 \pi^- \pi^+$  and  $B^0 \rightarrow D^{*-} K^+ \rightarrow \bar{D}^0 \pi^- K^+$ . One can find that the branching ratios of the modes with a pion bachelor meson are one power larger than their corresponding ones with a kaon bachelor meson. The reason is that the pion bachelor modes are the Cabibbo favored ( $V_{ud}$ ) processes, while the kaon bachelor modes are Cabibbo suppressed ( $V_{us}$ ) ones. The branching ratios of the Cabibbo favored decays  $B_s^0 \rightarrow D_s^{*-} \pi^+ \rightarrow \bar{D}^0 K^- \pi^+$  and  $B_s^0 \rightarrow \bar{D}^{*0} \bar{K}^0 \rightarrow \bar{D}^0 \pi^0 \bar{K}^0$  shown in Table V are larger than those of the remaining Cabibbo suppressed decays.

Similar to the dynamics in two-body hadronic  $B$  decays, the color favored tree ( $T$ ) topological diagram is absolutely dominating. Branching fractions of decays with the  $T$  diagram are larger than those with only  $C$  or  $E$  diagrams. Our results for these branching fractions with the  $T$  diagram are in good agreement with the PQCD predictions [16]. We have  $|C| > |E|$  in the FAT approach [39], while  $|C| \sim |E|$  in the PQCD approach [58]. The  $|C|$  contributes larger in the FAT approach than in the PQCD approach. Therefore, our branching fractions of  $B^0 \rightarrow \bar{D}^{*0} K^0 \rightarrow \bar{D}^0 \pi^0 K^0$  and  $B_s^0 \rightarrow \bar{D}^{*0} \bar{K}^0 \rightarrow \bar{D}^0 \pi^0 \bar{K}^0$  decays with only the  $C$  diagram are about two times larger than that in the PQCD approach.

For those decays with exactly the same intermediate state  $D_{(s)}^* P_2$ , their hierarchies of the branching ratios are completely caused by the strong decays of  $D_{(s)}^* \rightarrow D_{(s)} P_1$ . There are two hierarchy sources. One is the BWT effect, and the other is the strong couplings. Some of the decays, labeled by  $\mathcal{B}$  in the tables, can proceed by the pole mass dynamics; i.e., the pole mass is larger than the invariant mass threshold of two final states. The others labeled by  $\mathcal{B}_v$  can only happen by the BWT effect. The branching ratios of  $\mathcal{B}$  mode decays are apparently one to two orders larger than those of  $\mathcal{B}_v$  mode decays. The difference due to strong couplings is also obvious. For

instance, the isospin relation leads to  $g_{D^{*-} \bar{D}^0 \pi^-} = -\sqrt{2} g_{D^{*-} D^- \pi^0}$ . As a result, the branching ratio of  $B_{(s)}^0 \rightarrow \bar{D}^0 \pi^- \pi^+ (K^+)$  is approximately two times larger than that of  $B_{(s)}^0 \rightarrow D^- \pi^0 \pi^+ (K^+)$ . The strong decays with a pair of  $s\bar{s}$  quarks from the sea proceed only by the BWT effect because of the heavy strange quark mass. Consequently, the corresponding branching fractions are smaller than the others.

## B. Dependence of branching fractions on the invariant mass of intermediate state

We take the decays  $B^+ \rightarrow \bar{D}^{*0} \pi^+ \rightarrow \bar{D}^0 \pi^0 (D^- \pi^+, D_s^- K^+) \pi^+$  as an example to show the dependence of branching fractions on the invariant mass of  $\bar{D}^0 \pi^0$  pair (or  $D^- \pi^+, D_s^- K^+$ ), which is depicted in the left diagram of Fig. 2. To demonstrate the flavor  $SU(3)$  symmetry breaking effect, curves of their corresponding decays with the bachelor pion replaced with the kaon are plotted in the right diagram of Fig. 2. The decay with a pole mass dynamical strong decay  $\bar{D}^{*0} \rightarrow \bar{D}^0 \pi^0$  and those with the BWT effect strong decays  $\bar{D}^{*0} \rightarrow D^- \pi^+$  and  $\bar{D}^{*0} \rightarrow D_s^- K^+$  are represented by solid (red) lines, dashed (blue) lines, and dot-dashed (green) lines, respectively. Data of the decays with  $\bar{D}^{*0} \rightarrow D_s^- K^+$ , which are 1 order of magnitude smaller than those with  $\bar{D}^{*0} \rightarrow D^- \pi^+$ , are multiplied by 10 in order to be shown clearly on the same figure. One may notice the two conspicuous flagpoles located at the mass of  $\bar{D}^{*0}$  in Fig. 2. It is the distinguishing characteristic of pole dynamics. Our curves of  $B^+ \rightarrow \bar{D}^{*0} \pi^+ \rightarrow \bar{D}^0 \pi^0 (D^- \pi^+, D_s^- K^+) \pi^+$  (the red solid lines) have higher peaks than that from the ones in the PQCD approach [16], which indicates the pole mass dynamics plays a more important role in our results.

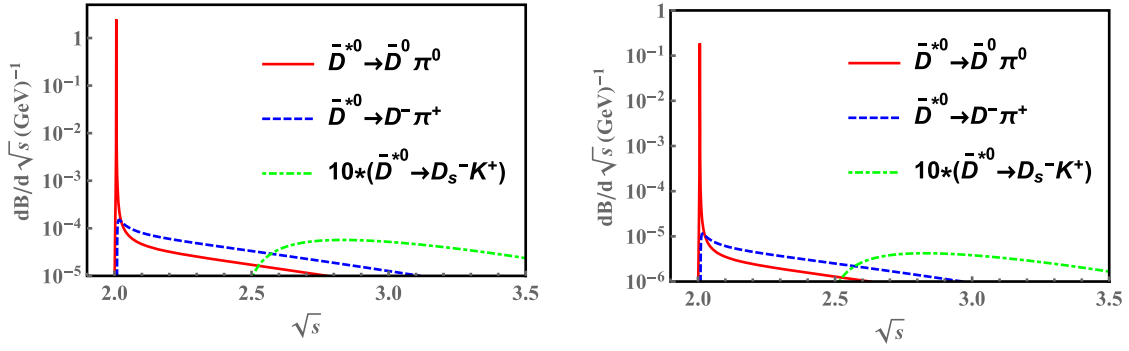


FIG. 2. The differential branching fractions of  $B^+ \rightarrow \bar{D}^{*0} \pi^+ \rightarrow \bar{D}^0 \pi^0 (D^- \pi^+, D_s^- K^+) \pi^+$  decays (left panel) and corresponding decays with the bachelor pion replaced with the kaon (right panel).

Only a few charmed three-body  $B$  decays are measured by the experiments. We collected these channels in Table VI as well as the results of the PQCD approach. Our results are consistent with the PQCD ones except the decay  $B_s^0 \rightarrow D_s^{*-} \pi^+ \rightarrow \bar{D}^0 K^- \pi^+$ . However, the experimental data of this decay have a very large uncertainty. It may be a good choice to wait for more accurate experimental measurement. Our calculation of the intermediate decays  $B \rightarrow D_{(s)}^* P$  is more precise than the PQCD approach, especially for the color suppressed (C) or exchange decay amplitudes (E) as these two nonfactorizable amplitudes,  $C$  and  $E$ , are fitted from precise experiment data in FAT not calculated perturbatively. Therefore, our theoretical uncertainty is much smaller than the previous PQCD approach. We also study the BWT effects in these decays. Although the  $B_s$  decay in Table VI has only BWT contribution, the four decays of  $B^{+,0}$  are dominated by pole dynamics. To make an effective comparison, the BWT effects of  $B^{+,0}$  decays are calculated with a cut of  $\sqrt{s} \geq 2.1$  GeV, which is also adopted by experiments and the PQCD approach. Comparing the data in Tables VI and IV, one can see that the BWT effect contributes about 5% in  $B^0$ -meson decays. For example, the center value of the branching ratio of  $B^0 \rightarrow D^{*-} \pi^+ \rightarrow \bar{D}^0 \pi^- \pi^+$  in Tables VI by a cut of  $\sqrt{s} \geq 2.1$  GeV in FAT is  $10.26 \times 10^{-5}$ , and the one in the whole

physical region of the  $\bar{D}^0 \pi^-$  invariant mass IV is  $1.77 \times 10^{-3}$ , which lead to the percentage of BWT effect being  $10.26 \times 10^{-5} / 1.77 \times 10^{-3} \sim 5\%$ .

Comparing the BWT effects of  $B^+ \rightarrow \bar{D}^{*0} \pi^+ \rightarrow D^- \pi^+ \pi^+$  and  $B^+ \rightarrow \bar{D}^{*0} \pi^+ \rightarrow D_s^- K^+ \pi^+$ , we find that the peaks of the green (dot-dashed) lines are located farther from the pole mass of  $\bar{D}^{*0}$  than the peaks of the blue (dashed) lines in Fig. 2. The reason is that  $D_s^- K^+$  has much larger threshold mass than  $D^- \pi^+$ . It can also be seen that the green (dot-dashed) line is smoother than the blue (dashed) line, which is very steep in the vicinity of the pole mass. Our calculation shows that the BWT effect in  $B^+ \rightarrow \bar{D}^{*0} \pi^+ \rightarrow D^- \pi^+ \pi^+$  is about 4%.

To check the dependence of the BWT effect on the widths of the intermediate resonance, we can compare those decays with different intermediate states. For instance, we find that contribution of the BWT effect is  $(1.64^{+0.36}_{-0.32}) \times 10^{-5}$  for  $B^0 \rightarrow D^{*-} \pi^+ \rightarrow D_s^- K^0 \pi^+$ ,  $(3.21^{+0.54}_{-0.50}) \times 10^{-5}$  for  $B^+ \rightarrow \bar{D}^{*0} \pi^+ \rightarrow D_s^- K^+ \pi^+$ , and  $(4.21^{+0.89}_{-0.81}) \times 10^{-5}$  for  $B_s^0 \rightarrow D_s^{*-} \pi^+ \rightarrow \bar{D}^0 K^- \pi^+$ . Their BWT effects are at the same order even though the widths of the resonances vary widely with  $\Gamma_{D^{*+}} = 83.4 \pm 1.8$  keV,  $\Gamma_{D^{*0}} = 55.3 \pm 1.4$  keV, and  $\Gamma_{D_s^*} \simeq 1$  keV. It indicates that the BWT effects in these decays are not very sensitive to the widths of resonances, which is

TABLE VI. The comparison of BWT effects between FAT, PQCD predictions, and available experimental measurements, where  $\mathcal{B}_{\text{FAT,PQCD}}^{\text{cut}}$  represents a cut on the invariant mass for  $B^{+,0}$  decays.

Decay modes	$\mathcal{B}_{\text{FAT}}^{\text{cut}} (10^{-5})$	$\mathcal{B}_{\text{PQCD}}^{\text{cut}} (10^{-5})$ [14]	Data ( $10^{-5}$ )
$B^+ \rightarrow \bar{D}^{*0} \pi^+ \rightarrow D^- \pi^+ \pi^+$	$18.8^{+3.16}_{-2.96}$	$19.2^{+8.80}_{-6.20}$	$22.3 \pm 3.20$ [59] $10.9 \pm 1.8$ [60] $10.9 \pm 2.7$ [30]
$B^+ \rightarrow \bar{D}^{*0} K^+ \rightarrow D^- \pi^+ K^+$	$1.39^{+0.24}_{-0.21}$	$1.48^{+0.68}_{-0.47}$	$0.56 \pm 0.23$ [47]
$B^0 \rightarrow D^{*-} \pi^+ \rightarrow \bar{D}^0 \pi^- \pi^+$	$10.26^{+2.25}_{-2.02}$	$8.7^{+4.5}_{-2.9}$	$8.8 \pm 1.3$ [26] $7.8$ [29]
$B^0 \rightarrow D^{*-} K^+ \rightarrow \bar{D}^0 \pi^- K^+$	$0.83^{+0.17}_{-0.15}$	$0.72^{+0.36}_{-0.24}$	$0.81 \pm 0.38$ [28]
$B_s^0 \rightarrow D_s^{*-} \pi^+ \rightarrow \bar{D}^0 K^- \pi^+$	$4.21^{+0.89}_{-0.81}$	$1.90^{+1.01}_{-0.68}$	$4.70 \pm 4.38$ [32]

confirmed by the PQCD approach [14,16]. This can be explained by the behavior of the Breit-Wigner propagators in the kinematics regions of these decays, where the real parts of their denominators are much larger than the imaginary parts. Taking  $D_s^{*-} \rightarrow \bar{D}^0 K^-$  as an example, the kinematics region starts from  $\sqrt{s} = 2.359$  GeV, while  $\Gamma_{D_s^{*-}} \simeq 1$  keV. It is obvious that  $|m_{D_s^{*-}}^2 - s| \gg |m_{D_s^{*-}} \Gamma_{D_s^{*-}}(s)|$ .

### C. Flavor $SU(3)$ symmetry breaking

Now, we turn to discuss the flavor- $SU(3)$  symmetry breaking effect in the quasi-two-body decays  $B^+ \rightarrow \bar{D}^{*0} \pi^+(K^+) \rightarrow \bar{D}^0 \pi^0 \pi^+(K^+)$  and  $B^0 \rightarrow D^{*-} \pi^+(K^+) \rightarrow \bar{D}^0 \pi^- \pi^+(K^+)$  with different bachelor particles  $\pi$  and  $K$ . The ratio of the branching fractions,

$$\begin{aligned} R_{D^{*-}} &= \frac{\mathcal{B}(\bar{B}^0 \rightarrow D^{*-} K^+ \rightarrow \bar{D}^0 \pi^- K^+)}{\mathcal{B}(\bar{B}^0 \rightarrow D^{*-} \pi^+ \rightarrow \bar{D}^0 \pi^- \pi^+)}, \\ R_{D^{*0}} &= \frac{\mathcal{B}(B^+ \rightarrow \bar{D}^{*0} K^+ \rightarrow \bar{D}^0 \pi^0 K^+)}{\mathcal{B}(B^+ \rightarrow \bar{D}^{*0} \pi^+ \rightarrow \bar{D}^0 \pi^0 \pi^+)}, \end{aligned} \quad (16)$$

can be used to test  $SU(3)$  symmetry breaking. Substituting the results in Table IV into the above equations, one gets

$$R_{D^{*-}} = 0.0831_{-0.0006}^{+0.0008}, \quad R_{D^{*0}} = 0.0761 \pm 0.0001. \quad (17)$$

$R_{D^{*-}}$  is consistent with the value  $(0.081_{-0.002}^{+0.000}(\omega_B)_{-0.000}^{+0.001}(a_{D\pi}))$  in the PQCD approach [14],  $(7.76 \pm 0.34 \pm 0.29)\%$  measured by the *BABAR* Collaboration [61], and  $(0.074 \pm 0.015 \pm 0.006)$  measured by the Belle Collaboration [62].  $R_{D^{*0}}$  also agrees well with the PQCD result of  $R_{D^{*0}} = 0.077_{-0.001}^{+0.000}(\omega_B)_{-0.001}^{+0.000}(\omega_{D\pi})$  [14] and the experimental data  $R_{D^{*0}} = 0.0813 \pm 0.0040(\text{stat})_{-0.0031}^{+0.0042}(\text{syst})$  [63]. The above ratios  $R_{D^{*-}} \simeq R_{D^{*0}} \simeq |V_{us}/V_{ud}|^2 \times (f_K/f_\pi)^2 = 0.076$ , which indicates that the source of  $SU(3)$  asymmetries are mainly from decay constants or weak transition form factors.

It is expected that the  $SU(3)$  symmetry breaking effect in the quasi-two-body decays should be equal to the

breaking effect calculated with their intermediate two-body decays

$$\begin{aligned} R_{D^{*0}} &= \frac{\mathcal{B}(B^+ \rightarrow \bar{D}^{*0} K^+ \rightarrow \bar{D}^0 \pi^0 K^+)}{\mathcal{B}(B^+ \rightarrow \bar{D}^{*0} \pi^+ \rightarrow \bar{D}^0 \pi^0 \pi^+)} \\ &\simeq \frac{\mathcal{B}(B^+ \rightarrow \bar{D}^{*0} K^+)}{\mathcal{B}(B^+ \rightarrow \bar{D}^{*0} \pi^+)}. \end{aligned} \quad (18)$$

This conclusion can be obtained with the narrow width approximation, under which one has

$$\begin{aligned} \mathcal{B}[B^+ \rightarrow \bar{D}^{*0} \pi^+(K^+) \rightarrow \bar{D}^0 \pi^0 \pi^+(K^+)] \\ \approx \mathcal{B}[B^+ \rightarrow \bar{D}^{*0} \pi^+(K^+)] \cdot \mathcal{B}[\bar{D}^{*0} \rightarrow \bar{D}^0 \pi^0]. \end{aligned} \quad (19)$$

Equation (18) can be checked numerically. Using the branching fractions calculated with the FAT approach [39],

$$\begin{aligned} \mathcal{B}(B^+ \rightarrow \bar{D}^{*0} K^+) &= (3.8_{-0.4}^{+0.6}) \times 10^{-4}, \\ \mathcal{B}(B^+ \rightarrow \bar{D}^{*0} \pi^+) &= (50.7_{-8.2}^{+8.1}) \times 10^{-4}, \end{aligned} \quad (20)$$

one gets

$$\frac{\mathcal{B}(B^+ \rightarrow \bar{D}^{*0} K^+)}{\mathcal{B}(B^+ \rightarrow \bar{D}^{*0} \pi^+)} = 0.0750 \pm 0.0001. \quad (21)$$

This value agrees with the  $R_{D^{*0}}$  in Eq. (17), which indicates that the narrow width approximation works very well in these decays.

Besides, the above conclusion can also be checked by the local  $SU(3)$  breaking effects, which are defined as the ratios of corresponding differential branching fractions on the invariant mass of  $\bar{D}^0 \pi^-$  or  $\bar{D}^0 \pi^0$ . Our results are plotted in Fig. 3. It can be seen that the magnitudes of the  $SU(3)$  symmetry breaking at every physical point are approximately equal.

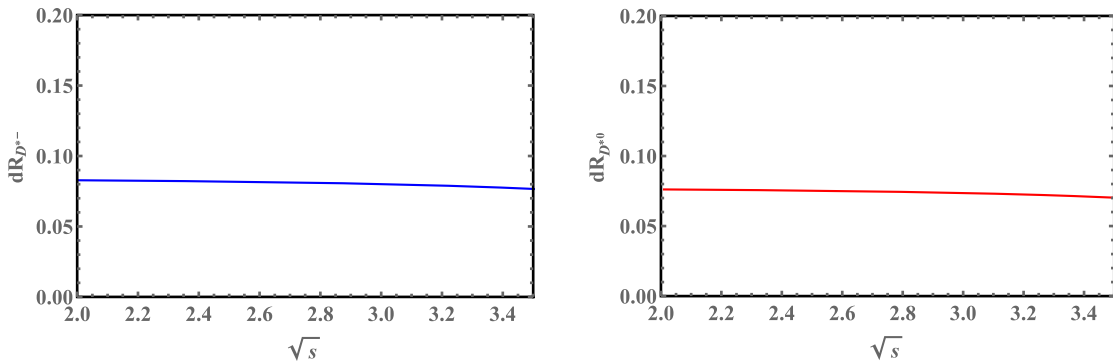


FIG. 3. The plotted curves are the ratios of corresponding differential branching fractions as functions of the invariant mass of  $\bar{D}^0 \pi^-$  or  $\bar{D}^0 \pi^0$ . These ratios could be defined as  $dR_{D^{*-}}$  or  $dR_{D^{*0}}$ , which could be the y labels.



#### IV. CONCLUSION

The three-body charmed  $B$ -meson decays are dominated by intermediate resonances; i.e., they proceed via quasi-two-body decays as  $B_{(s)} \rightarrow D_{(s)}^* P_2 \rightarrow D_{(s)} P_1 P_2$ . The first step of two-body decay is induced by flavor changing weak decays  $b \rightarrow cq\bar{u}$  ( $q = d, s$ ), and the intermediate resonant state  $D_{(s)}^*$  successively decays into  $D_{(s)} P_1$  via strong interaction. We utilize the decay amplitudes extracted from the two-body charmed  $B$  decays to quasi-two-body decays with the intermediate resonance described by the Breit-Wigner propagator. Including all the  $P$ -wave resonant states  $\bar{D}_{(s)}^*$ , we systematically study these decays. The  $B_{(s)} \rightarrow D_{(s)}^* P_2 \rightarrow D_{(s)} P_1 P_2$  decays can be divided into two groups:  $\mathcal{B}$  and  $\mathcal{B}_v$ .  $\mathcal{B}$  represents the group of decays whose pole mass of the resonance  $\bar{D}_{(s)}^*$  is larger than the threshold mass of producing  $\bar{D}_{(s)} P_1$ . This group of decays is dominated by the pole dynamics, and the main contributions to their branching fractions are from vicinity of the resonances' pole masses. The others labeled by  $\mathcal{B}_v$  can only happen with the BWT effect. The BWT effects in  $B^0$  decays are approximately 5%. We also found that the Breit-Wigner tail effects are not sensitive to the widths of their corresponding resonances.

We compare our results of the branching fractions with the PQCD approach's predictions as well as the experimental data. The largest theoretical uncertainty in the calculation is from the intermediate two-body charmed

$B$ -meson decays. Since this calculation is done by a global fit to all experimental data, our results of three-body  $B$  decays have significantly less theoretical uncertainty than the PQCD calculation. We use the same cut on the kinematics region of those decays proceeding via pole dynamics as the experiments. Our results agree well with the experimental data. For those ones without any experimental data, we would like to confront them with the future more accurate experiment measurements.

The flavor- $SU(3)$  symmetry breaking effect in these decays is studied. Our results  $R_{D^{*-}} = 0.0831_{-0.0006}^{+0.0008}$  and  $R_{D^{*0}} = 0.0761 \pm 0.0001$  are perfectly consistent with their experimental values. Besides, the local  $SU(3)$ -breaking effects, which are defined as ratios of corresponding differential branching fractions, are investigated. Their magnitudes are found not sensitive to the invariant mass of the strong decay final states, which confirms the that the  $SU(3)$  asymmetry in three-body decays is dominated by the two-body weak decays.

#### ACKNOWLEDGMENTS

We are grateful to Wen-Fei Wang for useful discussion. The work is supported by the National Natural Science Foundation of China under Grants No. 11765012, No. 12075126, No. 11521505, No. 11621131001, and No. 12105148 and National Key Research and Development Program of China under Contract No. 2020YFA0406400.

- 
- [1] M. Beneke, G. Buchalla, M. Neubert, and C. T. Sachrajda, QCD factorization for exclusive, nonleptonic B meson decays: General arguments and the case of heavy light final states, *Nucl. Phys.* **B591**, 313 (2000).
  - [2] C. D. Lu, K. Ukai, and M. Z. Yang, Branching ratio and  $CP$  violation of  $B \rightarrow \pi\pi$  decays in perturbative QCD approach, *Phys. Rev. D* **63**, 074009 (2001).
  - [3] C. W. Bauer, S. Fleming, D. Pirjol, and I. W. Stewart, An effective field theory for collinear and soft gluons: Heavy to light decays, *Phys. Rev. D* **63**, 114020 (2001).
  - [4] H. n. Li, C. D. Lü, and F. S. Yu, Branching ratios and direct  $CP$  asymmetries in  $D \rightarrow PP$  decays, *Phys. Rev. D* **86**, 036012 (2012).
  - [5] H. Y. Cheng and K. C. Yang, Nonresonant three-body decays of D and B mesons, *Phys. Rev. D* **66**, 054015 (2002).
  - [6] H. Y. Cheng, C. K. Chua, and A. Soni, Charmless three-body decays of B mesons, *Phys. Rev. D* **76**, 094006 (2007).
  - [7] H. Y. Cheng and C. K. Chua, Branching fractions and direct  $CP$  violation in charmless three-body decays of B mesons, *Phys. Rev. D* **88**, 114014 (2013).
  - [8] S. Fajfer, T. N. Pham, and A. Prapotnik,  $CP$  violation in the partial width asymmetries for  $B \rightarrow \pi^+ \pi^- K^-$  and  $B \rightarrow K^+ K^- K^-$  decays, *Phys. Rev. D* **70**, 034033 (2004).
  - [9] C. H. Chen and H. n. Li, Three body nonleptonic B decays in perturbative QCD, *Phys. Lett. B* **561**, 258 (2003).
  - [10] W. F. Wang, H. C. Hu, H. n. Li, and C. D. Lü, Direct  $CP$  asymmetries of three-body  $B$  decays in perturbative QCD, *Phys. Rev. D* **89**, 074031 (2014).
  - [11] W. F. Wang, H. n. Li, W. Wang, and C. D. Lü,  $S$ -wave resonance contributions to the  $B_{(s)}^0 \rightarrow J/\psi \pi^+ \pi^-$  and  $B_s \rightarrow \pi^+ \pi^- \mu^+ \mu^-$  decays, *Phys. Rev. D* **91**, 094024 (2015).
  - [12] W. F. Wang and H. n. Li, Quasi-two-body decays  $B \rightarrow K\rho \rightarrow K\pi\pi$  in perturbative QCD approach, *Phys. Lett. B* **763**, 29 (2016).
  - [13] A. J. Ma, Y. Li, W. F. Wang, and Z. J. Xiao, The quasi-two-body decays  $B_{(s)} \rightarrow (D_{(s)}, \bar{D}_{(s)})\rho \rightarrow (D_{(s)}, \bar{D}_{(s)})\pi\pi$  in the perturbative QCD factorization approach, *Nucl. Phys.* **B923**, 54 (2017).
  - [14] W. F. Wang and J. Chai, Virtual contributions from  $D^*(2007)^0$  and  $D^*(2010)^\pm$  in the  $B \rightarrow D\pi h$  decays, *Phys. Lett. B* **791**, 342 (2019).

- [15] W. F. Wang, Will the subprocesses  $\rho(770, 1450)^0 \rightarrow K^+K^-$  contribute large branching fractions for  $B^\pm \rightarrow \pi^\pm K^+K^-$  decays?, *Phys. Rev. D* **101**, 111901(R) (2020).
- [16] J. Chai, S. Cheng, and W. F. Wang, The role of  $D_{(s)}^*$  and their contributions in  $B_{(s)} \rightarrow D_{(s)}hh'$  decays, *Phys. Rev. D* **103**, 096016 (2021).
- [17] T. Huber, J. Virto, and K. K. Vos, Three-body non-leptonic heavy-to-heavy  $B$  decays at NNLO in QCD, *J. High Energy Phys.* **11** (2020) 103.
- [18] S. Kränkl, T. Mannel, and J. Virto, Three-body non-leptonic  $B$  decays and QCD factorization, *Nucl. Phys.* **B899**, 247 (2015).
- [19] T. Mannel, K. Olschewsky, and K. K. Vos,  $CP$  violation in three-body  $B$  decays: A model ansatz, *J. High Energy Phys.* **06** (2020) 073.
- [20] M. Gronau and J. L. Rosner, Symmetry relations in charmless  $B \rightarrow PPP$  decays, *Phys. Rev. D* **72**, 094031 (2005).
- [21] D. Xu, G. N. Li, and X. G. He, U-spin analysis of  $CP$  violation in  $B^-$  decays into three charged light pseudoscalar mesons, *Phys. Lett. B* **728**, 579 (2014).
- [22] G. Engelhard, Y. Nir, and G. Raz, SU(3) relations and the  $CP$  asymmetry in  $B \rightarrow K(S)K(S)K(S)$ , *Phys. Rev. D* **72**, 075013 (2005).
- [23] M. Imbeault and D. London, SU(3) breaking in charmless  $B$  decays, *Phys. Rev. D* **84**, 056002 (2011).
- [24] B. Bhattacharya, M. Gronau, and J. L. Rosner,  $CP$  asymmetries in three-body  $B^\pm$  decays to charged pions and kaons, *Phys. Lett. B* **726**, 337 (2013).
- [25] B. Bhattacharya, M. Gronau, M. Imbeault, D. London, and J. L. Rosner, Charmless  $B \rightarrow PPP$  decays: The fully-symmetric final state, *Phys. Rev. D* **89**, 074043 (2014).
- [26] A. Kuzmin *et al.* (BELLE Collaboration), Study of anti- $B^0 \rightarrow D^0\pi^+\pi^-$  decays, *Phys. Rev. D* **76**, 012006 (2007).
- [27] R. Aaij *et al.* (LHCb Collaboration), First observation and amplitude analysis of the  $B^- \rightarrow D^+K^-\pi^-$  decay, *Phys. Rev. D* **91**, 092002 (2015); **93**, 119901(E) (2016).
- [28] R. Aaij *et al.* (LHCb Collaboration), Amplitude analysis of  $B^0 \rightarrow \bar{D}^0K^+\pi^-$  decays, *Phys. Rev. D* **92**, 012012 (2015).
- [29] R. Aaij *et al.* (LHCb Collaboration), Dalitz plot analysis of  $B^0 \rightarrow \bar{D}^0\pi^+\pi^-$  decays, *Phys. Rev. D* **92**, 032002 (2015).
- [30] R. Aaij *et al.* (LHCb Collaboration), Amplitude analysis of  $B^- \rightarrow D^+\pi^-\pi^-$  decays, *Phys. Rev. D* **94**, 072001 (2016).
- [31] J. Wiechczynski *et al.* (BELLE Collaboration), Measurement of  $B^0 \rightarrow D_s^-K_S^0\pi^+$  and  $B^+ \rightarrow D_s^-K^+K^+$  branching fractions, *Phys. Rev. D* **91**, 032008 (2015).
- [32] R. Aaij *et al.* (LHCb Collaboration), Dalitz plot analysis of  $B_s^0 \rightarrow \bar{D}^0K^-\pi^+$  decays, *Phys. Rev. D* **90**, 072003 (2014).
- [33] A. Le Yaouanc, J. P. Leroy, and P. Roudeau, Large off-shell effects in the  $\bar{D}^*$  contribution to  $B \rightarrow \bar{D}\pi\pi$  and  $B \rightarrow \bar{D}\pi\bar{\nu}_\ell$  decays, *Phys. Rev. D* **99**, 073010 (2019).
- [34] M. Bauer, B. Stech, and M. Wirbel, Exclusive nonleptonic decays of  $D$ ,  $D(s)$ , and  $B$  mesons, *Z. Phys. C* **34**, 103 (1987).
- [35] A. Deandrea, N. Di Bartolomeo, R. Gatto, and G. Nardulli, Two body non leptonic decays of  $B$  and  $B_s$  mesons, *Phys. Lett. B* **318**, 549 (1993).
- [36] K. Azizi, R. Khosravi, and F. Falahati, Analyzing of the  $B(q) \rightarrow D(q)(D^*(q))P$  and  $B(q) \rightarrow D(q)(D^*(q))V$  decays within the factorization approach in QCD, *Int. J. Mod. Phys. A* **24**, 5845 (2009).
- [37] T. Kurimoto, H. n. Li, and A. I. Sanda,  $B \rightarrow D^{(*)}$  form factors in perturbative QCD, *Phys. Rev. D* **67**, 054028 (2003).
- [38] Y. Y. Keum, T. Kurimoto, H. n. Li, C. D. Lü, and A. I. Sanda, Nonfactorizable contributions to  $B \rightarrow D^{(*)}M$  decays, *Phys. Rev. D* **69**, 094018 (2004).
- [39] S. H. Zhou, Y. B. Wei, Q. Qin, Y. Li, F. S. Yu, and C. D. Lü, Analysis of two-body charmed  $B$  meson decays in factorization-assisted topological-amplitude approach, *Phys. Rev. D* **92**, 094016 (2015).
- [40] H. Y. Cheng, C. W. Chiang, and A. L. Kuo, Updating  $B \rightarrow PP, VP$  decays in the framework of flavor symmetry, *Phys. Rev. D* **91**, 014011 (2015).
- [41] Q. Qin, H. n. Li, C. D. Lü, and F. S. Yu, Branching ratios and direct  $CP$  asymmetries in  $D \rightarrow PV$  decays, *Phys. Rev. D* **89**, 054006 (2014).
- [42] S. H. Zhou, Q. A. Zhang, W. R. Lyu, and C. D. Lü, Analysis of charmless two-body  $B$  decays in factorization assisted topological amplitude approach, *Eur. Phys. J. C* **77**, 125 (2017).
- [43] H. Y. Jiang, F. S. Yu, Q. Qin, H. n. Li, and C. D. Lü,  $D^0 - \bar{D}^0$  mixing parameter  $\gamma$  in the factorization-assisted topological-amplitude approach, *Chin. Phys. C* **42**, 063101 (2018).
- [44] S. H. Zhou and C. D. Lü, Extraction of the CKM phase  $\gamma$  from the charmless two-body  $B$  meson decays, *Chin. Phys. C* **44**, 063101 (2020).
- [45] J. Blatt and V. Weisskopf, *Theoretical Nuclear Physics* (John Wiley & Sons, New York, 1952).
- [46] R. Aaij *et al.* (LHCb Collaboration), Dalitz plot analysis of  $B_s^0 \rightarrow \bar{D}^0K^-\pi^+$  decays, *Phys. Rev. D* **90**, 072003 (2014).
- [47] R. Aaij *et al.* (LHCb Collaboration), First observation and amplitude analysis of the  $B^- \rightarrow D^+K^-K^-$  decay, *Phys. Rev. D* **91**, 092002 (2015).
- [48] P. A. Zyla *et al.* (Particle Data Group), Review of Particle Physics, *Prog. Theor. Exp. Phys.* **2020**, 083C01 (2020).
- [49] H. D. Li, C. D. Lü, C. Wang, Y. M. Wang, and Y. B. Wei, QCD calculations of radiative heavy meson decays with subleading power corrections, *J. High Energy Phys.* **04** (2020) 023.
- [50] G. C. Donald, C. T. H. Davies, J. Koponen, and G. P. Lepage, Prediction of the  $D_s^*$  Width from a Calculation of its Radiative Decay in Full Lattice QCD, *Phys. Rev. Lett.* **112**, 212002 (2014).
- [51] G. L. Yu, Z. Y. Li, and Z. G. Wang, Analysis of the strong coupling constant  $G_{D_s^*D_s\phi}$  and the decay width of  $D_s^* \rightarrow D_s\gamma$  with QCD sum rules, *Eur. Phys. J. C* **75**, 243 (2015).
- [52] B. Yang, B. Wang, L. Meng, and S. L. Zhu, Isospin violating decay  $D_s^* \rightarrow D_s\pi^0$  in chiral perturbation theory, *Phys. Rev. D* **101**, 054019 (2020).
- [53] J. P. Lees *et al.* (BABAR Collaboration), Measurement of the  $D^*(2010)^+$  natural line width and the  $D^*(2010)^+ - D^0$  mass difference, *Phys. Rev. D* **88**, 052003 (2013).
- [54] J. P. Lees *et al.* (BABAR Collaboration), Measurement of the  $D^{*+}(2010)$  Meson Width and the  $D^{*+}(2010) - D^0$  Mass Difference, *Phys. Rev. Lett.* **111**, 111801 (2013).
- [55] P. Colangelo and F. De Fazio, On three body  $B^0 \rightarrow D^* - D^{(*)0}K^+$  decays and couplings of heavy mesons to light pseudoscalar mesons, *Phys. Lett. B* **532**, 193 (2002).

- [56] A. Anastassov *et al.* (CLEO Collaboration), First measurement of  $\Gamma(D^{*+})$  and precision measurement of  $m(D^{*+})-m(D^0)$ , *Phys. Rev. D* **65**, 032003 (2002).
- [57] D. Becirevic and A. Le Yaouanc, G coupling ( $g(B^*B\pi)$ ,  $g(D^*D\pi)$ ): A quark model with Dirac equation, *J. High Energy Phys.* **03** (1999) 021.
- [58] R.H. Li, C.D. Lu, and H. Zou, The  $B(B_s) \rightarrow D(s)P, D(s)V, D^{*(s)}P$  and  $D^{*(s)}V$  decays in the perturbative QCD approach, *Phys. Rev. D* **78**, 014018 (2008).
- [59] K. Abe *et al.* (BELLE Collaboration), Study of  $B \rightarrow D^{**0}\pi^-(D^{**0} \rightarrow D^{(*)} + p\bar{i}^-)$  decays, *Phys. Rev. D* **69**, 112002 (2004).
- [60] B. Aubert *et al.* (BABAR Collaboration), Dalitz plot analysis of  $B \rightarrow D^+\pi^-\pi^-$  *Phys. Rev. D* **79**, 112004 (2009).
- [61] B. Aubert *et al.* (BABAR Collaboration), Measurement of Branching Fractions and Resonance Contributions for  $B^0 \rightarrow \bar{D}^0K^+\pi^-$  and Search for  $B^0 \rightarrow D^0K^+\pi^-$  Decays, *Phys. Rev. Lett.* **96**, 011803 (2006).
- [62] K. Abe *et al.* (BELLE Collaboration), Observation of Cabibbo Suppressed  $B \rightarrow D^{(*)}K^-$  Decays at BELLE, *Phys. Rev. Lett.* **87**, 111801 (2001).
- [63] B. Aubert *et al.* (BABAR Collaboration), Measurement of the ratio  $B(B^- \rightarrow D^{*0}K^-)/B(B^- \rightarrow D^{*0}\pi^-)$  and of the  $CP$  asymmetry of  $B^- \rightarrow D_{CP+}^{*0}K^-$  decays, *Phys. Rev. D* **71**, 031102 (2005).